

## The impact of ensemble filter definition on the assimilation of temperature profiles in the Tropical Pacific

By O. LEEUWENBURGH<sup>1\*</sup>, G. EVENSEN<sup>2,3</sup> and L. BERTINO<sup>3</sup>

<sup>1</sup>*Royal Netherlands Meteorological Institute (KNMI), De Bilt, the Netherlands*

<sup>2</sup>*Norsk Hydro, Bergen, Norway*

<sup>3</sup>*Nansen Environmental and Remote Sensing Center, Bergen, Norway*

(Received XXX; revised XXX)

### SUMMARY

The traditional analysis scheme in the Ensemble Kalman Filter (EnKF) uses a stochastic perturbation or randomization of the measurements which ensures a correct variance in the updated ensemble. An alternative deterministic analysis algorithm is based on a so called square-root formulation where the perturbation of measurements is avoided. Experiments with simple models have indicated that ensemble collapse is likely to occur when deterministic filters are applied to nonlinear problems. In this paper the properties of stochastic and deterministic ensemble analysis algorithms are evaluated in an identical-twin experiment using an ocean general circulation model. In particular, the implications of the use of deterministic ensemble square-root filters (EnSRF) for ensemble spread are investigated. An explanation is presented for the observed collapse and a simple solution based on randomization of the analysis ensemble anomalies is examined. A 1-year assimilation run with this improved EnSRF is found to produce Gaussian distributions, similar to the Ensemble Kalman Filter.

KEYWORDS: Ensemble Kalman Filter   Ensemble Square-Root Filter   Assimilation

### 1. INTRODUCTION

The Ensemble Kalman Filter (EnKF) provides a linear update to a non-linear forecast ensemble and can thus be viewed as an intermediate step between the Kalman Filter and particle filters. Investigations into its application to both atmospheric and oceanographic systems have shown significant improvements with respect to OI-type systems (Keppenne and Rienecker, 2002; Houtekamer *et al.*, 2005), and similar performance as currently operational 3DVar systems (Houtekamer *et al.*, 2005). The stochastic EnKF algorithm (Evensen, 1994; Burgers *et al.*, 1998) has properties and limitations which are by now well understood. Outstanding issues are primarily related to the maintenance of ensemble spread and balance for relatively small ensemble sizes, and the treatment of model bias.

Some recent studies have promoted deterministic filters on the grounds that they are expected to be more accurate and computationally more efficient, and preserve certain higher-order, non-Gaussian statistics of the forecast ensemble (Tippett *et al.*, 2003). Lawson and Hansen (2004) compared the behaviour of the EnKF with the deterministic Ensemble Square-Root Filter (EnSRF) of Whitaker and Hamill (2002) in linear and nonlinear dynamical regimes with simple test models. They noticed that while ensemble variance is formally maintained by the EnSRF, all members but one tend to collapse onto one state, with a single outlier providing the prescribed variance. The EnKF on the other hand tends to maintain a Gaussian ensemble spread also under nonlinear dynamical regimes due to the Gaussian form of the observation perturbations.

The question addressed here is to what extent these findings are relevant for realistic applications. In particular, we compare the behaviour of the EnKF and an EnSRF in an identical-twin experiment where temperature profiles are assimilated into the Tropical Pacific domain of an ocean general circulation model.

\* Corresponding author address: KNMI, PO Box 201, 3730 AE, De Bilt, The Netherlands. E-mail: leeuwenburgh@knmi.nl

© Royal Meteorological Society, 2004.

The assimilation algorithms are reviewed briefly in Section 2. The addition of a randomization step to the EnSRF algorithm is suggested as a means to counter the tendency for ensemble collapse. Section 3 gives a short overview of the experiment setup, including a description of the model. Results from 1-year assimilation runs with the EnKF, EnSRF, and the randomized EnSRF are presented in Section 4. Finally, Section 5 concludes with a summary and discussion.

## 2. ANALYSIS ALGORITHMS

The analysis algorithms discussed here are described in detail by Evensen (2004), but are now reviewed briefly. The EnSRF algorithm is explored in some more detail.

### (a) Ensemble Kalman Filter

The standard EnKF analysis algorithm (Evensen, 1994; Burgers *et al.*, 1998) is given by

$$\mathbf{A}^a = \mathbf{A} + \mathbf{P}\mathbf{H}^T(\mathbf{H}\mathbf{P}\mathbf{H}^T + \mathbf{R})^{-1}(\mathbf{D} - \mathbf{H}\mathbf{A}) \quad (1)$$

$$= \mathbf{A} + \mathbf{A}'\mathbf{A}'^T\mathbf{H}^T(\mathbf{H}\mathbf{A}'\mathbf{A}'^T\mathbf{H}^T + (N-1)\mathbf{R})^{-1}(\mathbf{D} - \mathbf{H}\mathbf{A}) \quad (2)$$

$$(3)$$

where  $\mathbf{A} = (\boldsymbol{\psi}_1, \dots, \boldsymbol{\psi}_N)$  holds the ensemble of model forecasts,  $\mathbf{H}$  is the measurement operator,  $\mathbf{R}$  is the observation error covariance matrix, and  $\mathbf{D}$  is the ensemble of perturbed measurements. Primes indicate anomalies with respect to the ensemble mean, and the ensemble covariances are defined by  $\mathbf{P} = \mathbf{A}'\mathbf{A}'^T/(N-1)$ .

### (b) Ensemble Square Root Filter

The EnSRF updates the ensemble mean and the anomalies separately. The updated mean,  $\overline{\boldsymbol{\psi}}^a$  is computed by an equation similar to (1), i.e.,

$$\overline{\boldsymbol{\psi}}^a = \overline{\boldsymbol{\psi}}^f + \mathbf{P}\mathbf{H}^T(\mathbf{H}\mathbf{P}\mathbf{H}^T + \mathbf{R})^{-1}(\mathbf{d} - \mathbf{H}\overline{\boldsymbol{\psi}}^f), \quad (4)$$

where  $\mathbf{d}$  are the unperturbed measurements. This gives exactly the same updated ensemble mean as the EnKF as long as the measurement perturbations average to zero.

An equation for the updated perturbations is obtained by equating the definition of the ensemble covariance matrix with the covariance update which follows from Kalman Filter theory,

$$\mathbf{P}^a = \mathbf{A}'^a\mathbf{A}'^{aT} = \mathbf{P}(\mathbf{I} - \mathbf{H}^T(\mathbf{H}\mathbf{P}\mathbf{H}^T + \mathbf{R})^{-1}\mathbf{H}\mathbf{P}) \quad (5)$$

$$= \mathbf{A}'(\mathbf{I} - \mathbf{S}^T\mathbf{C}^{-1}\mathbf{S})\mathbf{A}'^T \quad (6)$$

$$= \mathbf{A}'(\mathbf{I} - \mathbf{Z}\boldsymbol{\Lambda}\mathbf{Z}^T)\mathbf{A}'^T \quad (7)$$

$$= \mathbf{A}'\mathbf{Z}(\mathbf{I} - \boldsymbol{\Lambda})\mathbf{Z}^T\mathbf{A}'^T \quad (8)$$

$$= \left(\mathbf{A}'\mathbf{Z}\sqrt{\mathbf{I} - \boldsymbol{\Lambda}}\right)\left(\mathbf{A}'\mathbf{Z}\sqrt{\mathbf{I} - \boldsymbol{\Lambda}}\right)^T. \quad (9)$$

The notation  $\mathbf{S} = \mathbf{H}\mathbf{A}'$  and  $\mathbf{C} = \mathbf{S}\mathbf{S}^T + (N-1)\mathbf{R}$  is introduced in Eq. 6 and an eigen value decomposition of the second term within the brackets of Eq. 6 is

computed to obtain the eigenvectors  $\mathbf{Z}$  and eigenvalues  $\mathbf{\Lambda}$  (see Evensen (2004) for details). Thus we define the update equation for the ensemble perturbations as:

$$\mathbf{A}^{a'} = \mathbf{A}' \mathbf{Z} \sqrt{\mathbf{I} - \mathbf{\Lambda}}. \quad (10)$$

This is essentially the same equation as is solved in the EnSRF algorithms discussed in Tippett *et al.*, (2003) although they introduced additional simplifications for computational reasons.

A problem with the square-root filter algorithm can be illustrated by a simple example where a single observation is used with a scalar state. With a direct measurement operator  $\mathbf{H} = 1$  we have  $\mathbf{S} = \mathbf{A}'$ . Further, since only the first eigenvalue in  $\mathbf{\Lambda}$  is nonzero, then the first eigenvector in  $\mathbf{Z}$  must be identically proportional to  $\mathbf{S}^T$  (note that we have  $\mathbf{S} \in \mathfrak{R}^{1 \times N}$  in the case with a single measurement). This is seen from the equality between Eqs. (6) and (7). However, all the remaining  $N - 1$  eigenvectors are orthogonal to the first eigenvector, and thus also orthogonal to  $\mathbf{S}^T$ .

Thus, the update equation (10) will lead to an ensemble of updated perturbations where the first member will be equal to  $\mathbf{S}(\mathbf{S}^T / \|\mathbf{S}\|) \sqrt{1 - \lambda_1}$  and all the  $N - 1$  remaining perturbations will be identical to zero. Note that the resulting ensemble still has the correct variance, but it is determined by the perturbation in first ensemble member.

This example can clearly be extended to cases with larger state spaces. E.g., if the state dimension  $n > 1$  there will still be a problem at the measurement locations. In fact the rank of the ensemble is reduced to one at the measurement location.

With more than one measurement the situation changes slightly but the same problem will occur if  $\mathbf{C}^{-1}$  is diagonal. Then each of the  $m$  columns in  $\mathbf{S}^T$  will be proportional to one of the first  $m$  eigenvectors in  $\mathbf{Z}$ . Thus, the first  $m$  ensemble perturbations will represent the analysis variance while the remainder will be zero. This explains the findings of Lawson and Hansen (2004) where it was shown that the EnSRF tends to produce ensembles where the variance is provided by very few outliers.

The problem sketched here can be avoided by the insertion of a random orthogonal matrix product  $\mathbf{I} = \mathbf{V}^T \mathbf{V}$  in (9), as was proposed by Evensen (2004), i.e.,

$$\mathbf{A}^{a'} \mathbf{A}^{a'T} = \mathbf{A}' \mathbf{Z} \sqrt{\mathbf{I} - \mathbf{\Lambda}} \mathbf{V}^T \mathbf{V} \left( \mathbf{A}' \mathbf{Z} \sqrt{\mathbf{I} - \mathbf{\Lambda}} \right)^T \quad (11)$$

which leads to the following randomized EnSRF update equation

$$\mathbf{A}^{a'} = \mathbf{A}' \mathbf{Z} \sqrt{\mathbf{I} - \mathbf{\Lambda}} \mathbf{V}^T. \quad (12)$$

The multiplication with  $\mathbf{V}^T$  is equivalent to a random rotation of the eigenvectors in  $\mathbf{Z}$ , which has the effect of randomly distributing the variance reduction among all the ensemble members. The random orthogonal matrix  $\mathbf{V}^T$  is easily constructed from a singular value decomposition of a random matrix  $\mathbf{B} \in \mathfrak{R}^{N \times N}$ , i.e.  $\mathbf{B} = \mathbf{U} \mathbf{\Sigma} \mathbf{V}^T$ .

### (c) Localization

Following common practise, a covariance localisation step was added to the EnKF to reduce long-range spurious correlations and increase the dimension of

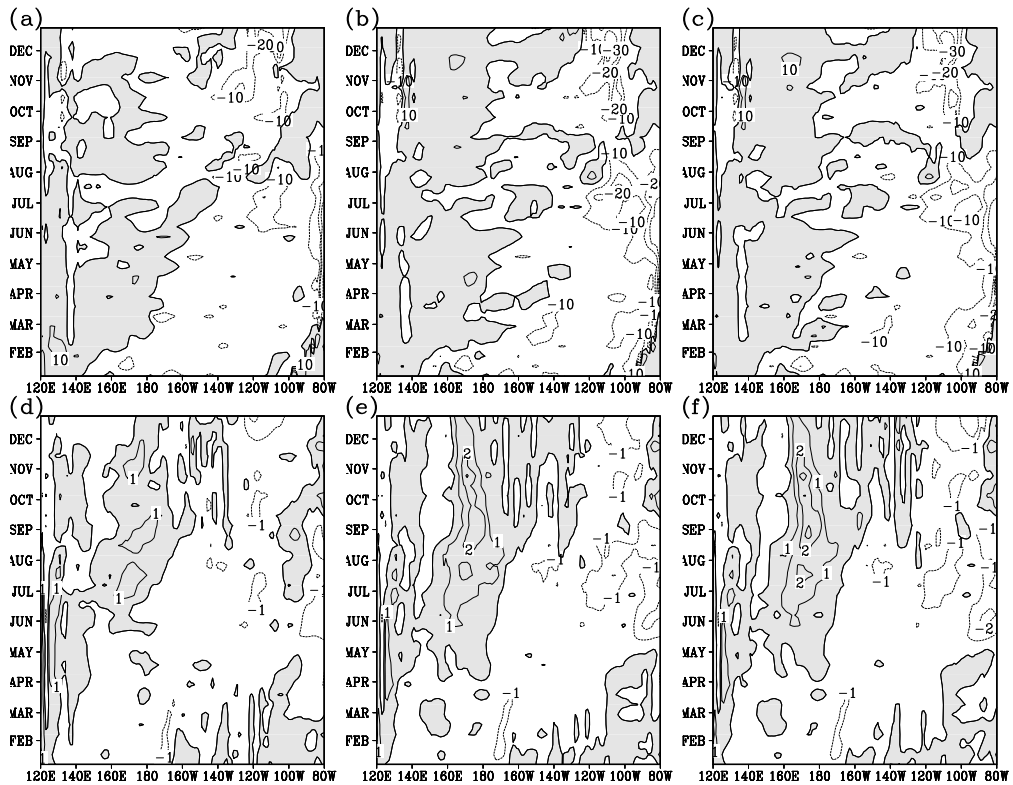


Figure 1. Differences between analysis and truth. (a) Z20 from EnKF, (b) Z20 from EnSRF, (c) Z20 from EnSRF with rotation, (d) T at 50m from EnKF, (e) T at 50m from EnSRF, (f) T at 50m from EnSRF with rotation.

the solution space (Houtekamer and Mitchell, 2001; Keppenne and Rienecker, 2002). Localisation was achieved for the EnSRF without covariance filtering by reducing the data selection range for each grid point, resulting in an approximately equivalent effective number of observations as for the EnKF.

### 3. EXPERIMENT SETUP

The ocean model that is used here is the Max Planck Institut für Meteorologie Ocean Model, or MPI-OM (Marsland *et al.* 2003). The model is run in a global configuration with meridional refinement of the grid ( $0.5^\circ$ ) within a  $20^\circ$  latitude band centered on the equator.

The true ocean state is defined by a forward run of the ocean model using NCEP/NCAR reanalysis forcing fields.

An unconstrained control run is forced with the ECMWF 40-year reanalysis (ERA40) forcing fields. The use of two different forcing products is meant to reflect the errors in our best-guess forcing products with respect to the true forcing. The initial ensemble at the start of the assimilation run consists of 64 model states which are obtained by a 1-year spinup of an ensemble with perturbed ERA40 forcing using the control state as initial condition. Details of the perturbation method can be found in Leeuwenburgh (2005).

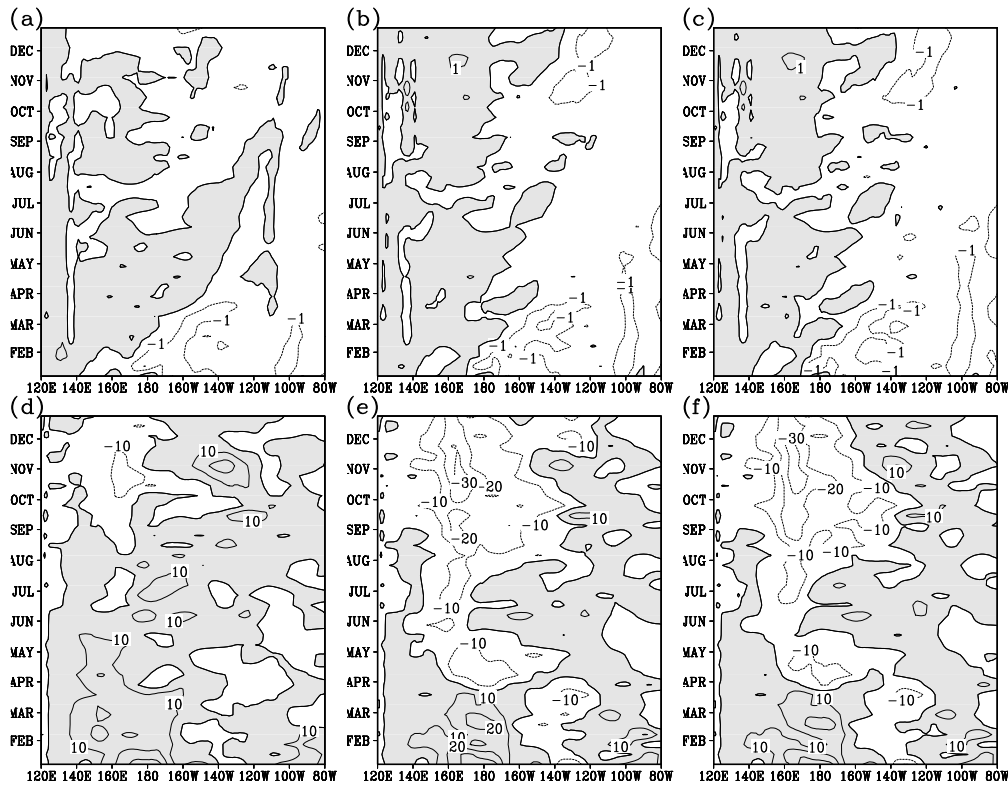


Figure 2. Differences between analysis and truth. (a) T at 150m from EnKF, (b) T at 150m from EnSRF, (c) T at 150m from EnSRF with rotation, (d) U at 75m from EnKF, (e) U at 75m from EnSRF, (f) U at 75m from EnSRF with rotation.

Temperature measurements were simulated by sampling the truth run at the geographical positions of the TAO (Tropical Atmosphere Ocean) buoys and the corresponding depths of the temperature sensors. Random perturbations with a  $1^{\circ}\text{C}$  standard deviation were added to all measurements to simulate realistic data errors.

The assimilation run lasts 12 months and consists of consecutive 10-day forward integrations of the ensemble (the resulting mean states will be referred to as the *forecasts*), each followed by a filter step during which the simulated observations are assimilated into the ensemble. The mean states of the resulting ensembles (the *analyses*) will be compared with the control and the truth to determine whether the assimilation has brought the model closer to the true state. The ensemble statistics resulting from the EnKF and EnSRF runs are compared to study the characteristics of the ensemble.

#### 4. RESULTS FROM ASSIMILATION RUNS

##### (a) Ensemble mean states

In this section the results are presented from 1-year assimilation runs performed with the EnKF and the EnSRF. A third run was performed in which the analysis ensemble anomalies resulting from the EnSRF undergo a random

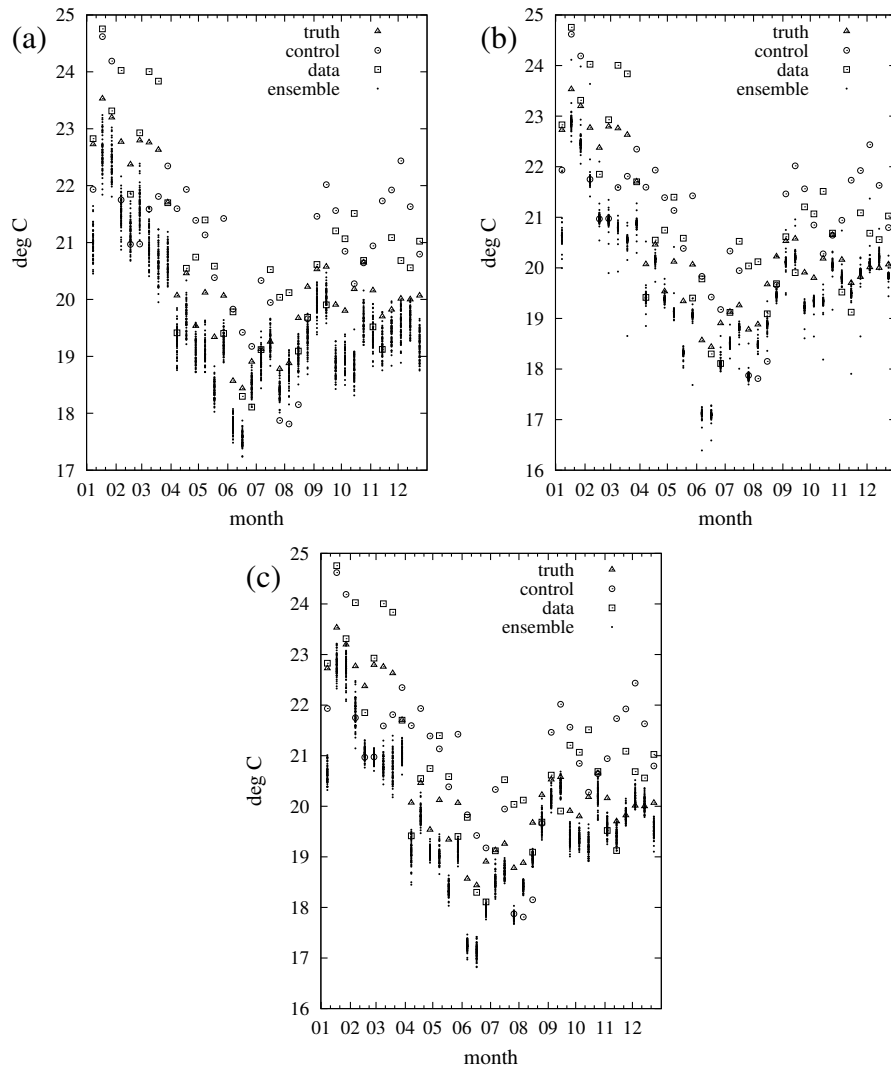


Figure 3. Temperature values at 220E 0N 120m depth from the truth, control, observations, and the ensembles obtained with (a) the EnKF, (b) the EnSRF, and (c) the EnSRF with rotation.

rotation as described in the section 2 (this run will be referred to as EnSRF+). Figures 1 and 2 show the time series of differences along the equator between analysis and truth for the depth of the 20°C isotherm (a good measure for the position of the thermocline near the equator), temperature at 50m and 150m depth, and zonal velocity at 75m depth. The figures indicate that the mean states have comparable quality. Perhaps surprisingly, the EnKF appears to have produced slightly better analyses. This runs contrary to the idea that the use of observation perturbations introduces noise leading to worse analyses. These figures can be compared to Figs. (6) and (7) from (Leeuwenburgh, 2005) which show the corresponding differences between control and truth and between a sea

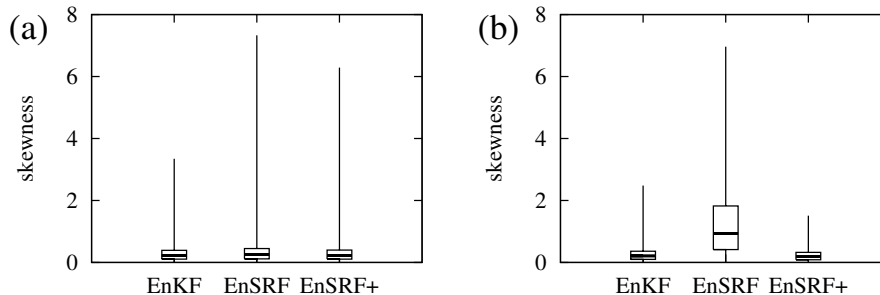


Figure 4. Ensemble skewness determined at observations points for (a) the forecast ensembles and (b) the analysis ensembles resulting from the assimilation runs with the EnKF, EnSRF and EnSRF with rotation (+). The box' bounds indicate the interquartile range, and the whiskers extend to the min and max values. The thick line indicates the median value. The maximum theoretical value is 7.75.

level assimilation run and the truth. The EnKF analyses resulting from temperature assimilation are consistently better than those resulting from sea level assimilation, while the EnSRF analyses are of comparable quality.

#### (b) Ensemble distribution

Figure 3 shows time series of the analyzed temperature at one of the measurement locations for all three runs. The small dots in these figures show the distribution of the individual members of the analysis ensembles. The three important observations that can be made on the basis of this figure are that (1) the EnSRF produces the same behaviour that was observed by Lawson and Hansen (2004), with in most cases only one outlier apparently providing the required variance; (2) the random rotation in the randomized version EnSRF+ produces an ensemble with a more even spread (3) the EnSRF+ members are grouped together more closely than those resulting from the EnKF.

The shape of the ensemble distribution can be assessed quantitatively using the skewness measure which is an indication of the asymmetry around the mean. Since a Gaussian distribution is symmetric, high skewness values indicate strong deviations from a Gaussian shape. The skewness of temperature values is determined at all measurement locations and at all time steps. Figure 4 shows for all three algorithms the resulting minimum and maximum values, the median, and the interquartile ranges found during each run. While the skewness values are very low for the EnKF and the EnSRF+, high values are obtained for the EnSRF, in agreement with the indications from the time series of Fig. 3. Since the forecast skewness estimates indicate fairly symmetric distributions, these high values must be a result of a deficiency of the EnSRF analysis algorithm.

Lawson and Hansen (2004) produced rank histograms as an additional tool to illustrate the high number of outliers. Hamill (2001) showed that rank histograms may indicate several deficiencies of the ensemble simultaneously, one of them being conditional biases which result in U-shaped histograms similar to those shown by Lawson and Hansen (2004). Ocean assimilation in the tropics may introduce biases on the equator through disturbance of the balance between the sea level gradient and surface wind stress (Bell *et al.*, 2004). Rank histograms may therefore not be the optimal tool for assessment of the ensemble distribution

in this case. Instead, a  $\chi^2$  test is performed here to determine whether the distributions are Gaussian or not. The temperature samples shown in Fig. 3 were binned into 6 classes relative to the ensemble mean values, each representing an equal area of the Gaussian PDF corresponding to the estimated standard deviation of ensemble spread. The sum of the squared differences between the number of occurrences in each class and the expected value (64/6) has a  $\chi^2$  distribution. The corresponding  $p$ -values are determined at every time step during the assimilation run. If the number of rejections of the Gaussian assumption, following from all individual  $\chi^2$  tests, exceeds a critical number associated with the binomial distribution and a chosen significance level, we conclude that the ensemble distributions are non-Gaussian. For the time series of Fig. 3 the Gaussian null-hypothesis is rejected at every time step for the EnSRF. The number of rejections for the EnKF and EnSRF+ is low enough that we can state with a 95% confidence level that the distributions are Gaussian.

## 5. SUMMARY AND CONCLUSIONS

Experiments are conducted to compare the behaviour of stochastic and deterministic ensemble filters in a realistic application. Simulated tropical temperature profiles are assimilated in an OGCM using Ensemble Kalman and Square-Root Filters. The mean analyzed states produced with the EnKF appear to be slightly better than those from the EnSRF. In agreement with Lawson and Hansen (2004) we find that the EnSRF has a tendency to collapse all but a few members onto a single state. Skewness measures and  $\chi^2$  tests confirm that the resulting ensembles are highly non-Gaussian.

These findings point to some fundamental problems with the EnSRF. Members of an ensemble should be equally likely, but the EnSRF returns singular vectors ordered by decreasing or increasing (depending on the algorithm) singular values (the square-root term in Eq. (10)). Given also that the sign of the vectors  $\mathbf{Z}$  is arbitrary, not all of the ensemble statistics are preserved. In particular the skewness observed with the EnSRF is most likely inherited from the skewness of the singular values (many near-zero singular values, few large values).

The EnSRF reduces errors along specific directions defined by  $\mathbf{Z}$  in Eq. (10), where  $\mathbf{Z}$  is a rotation which comes from the SVD of the product of the eigenvectors of  $\mathbf{C}$  and  $\mathbf{S}$ . Dependent on this product it is not clear what this will mean in different situations. The single observation and diagonal  $\mathbf{C}$  cases are just two cases where problems arise, and there may be more. In fact, even though all observations were assimilated simultaneously at each step, and a diagonal  $\mathbf{C}$  is unlikely to occur in realistic applications in oceanography and meteorology, similar behaviour was found to occur in our experiments.

An additional random rotation of the ensemble anomalies is found to fix the above problems well, although it was observed that the ensemble values are grouped together more closely than for the EnKF.

## REFERENCES

- |   |      |   |
|---|------|---|
| Bell, M. J., Martin, M. J. and Nichols, N. K.   | 2004 | Assimilation of data into an ocean model with systematic errors near the equator. <i>Q. J. R. Meteorol. Soc.</i> , <b>130</b> , 873–893 |
| Burgers, G., van Leeuwen, P. J. and Evensen, G. | 1998 | Analysis scheme in the Ensemble Kalman Filter. <i>Mon. Wea. Rev.</i> , <b>126</b> , 1719–1724   |

- Evensen, G. 1994 Sequential data assimilation with a nonlinear quasi-geostrophic model using Monte Carlo methods to forecast error statistics. *J. Geophys. Res.*, **C99**, 10143–10162
- Evensen, G. 2003 The ensemble Kalman Filter: theoretical formulation and practical implementation. *Ocean Dyn.*, **53**, 343–367
- Evensen, G. 2004 Sampling strategies and square root analysis schemes for the EnKF. *Ocean Dyn.*, **54**, 539–560
- Gaspari, G. and Cohn, S. E. 1999 Construction of correlation functions in two and three dimensions. *Q. J. R. Meteorol. Soc.*, **125**, 723–757
- Hamill, T. M. 2001 Interpretation of rank histograms for verifying ensemble forecasts. *Mon. Wea. Rev.*, **129**, 550–560
- Houtekamer, P. and Mitchell, H. 2001 A sequential Ensemble Kalman Filter for atmospheric data assimilation. *Mon. Wea. Rev.*, **129**, 123–137
- Houtekamer, P., Mitchell, H. L., Pellerin, G., Buehner, M., Charron, M., Spacek, L. and Hansen, B. 2005 Atmospheric data assimilation with an Ensemble Kalman Filter: results with real observations. *Mon. Wea. Rev.*, **133**, 604–620
- Keppenne, C. L. and Rienecker, M. M. 2002 Initial testing of a massively parallel Ensemble Kalman Filter with the Poseidon isopycnal ocean general circulation model. *Mon. Wea. Rev.*, **130**, 2951–2965
- Lawson, W. G. and Hansen, J. A. 2004 Implications of stochastic and deterministic filters as ensemble-based data assimilation methods in varying regimes of error growth. *Mon. Wea. Rev.*, **132**, 1966–1981
- Leeuwenburgh, O. 2005 Validation of an EnKF system for ocean initialisation assimilating temperature, salinity, and sea level measurements. *Mon. Wea. Rev.*, to appear
- Marsland, S., Haak, H., Jungclaus, J. H., Latif, M. and Röske, F. 2003 The Max-Planck-Institute global ocean/sea ice model with orthogonal curvilinear coordinates. *Ocean Modelling*, **5**, 91–127
- Tippett, M. K., Anderson, J. L., Bishop, C. H., Hamill, T. M. and Whitaker, J. S. 2003 Ensemble square root filters. *Mon. Wea. Rev.*, **131**, 1485–1490
- Whitaker, J. S. and Hamill, T. M. 2002 Ensemble data assimilation without perturbed observations. *Mon. Wea. Rev.*, **130**, 1913–1924